Influence of Impact Parameter on Thermal Description of Relativistic Heavy Ion Collisions at GSI/SIS.

Jean Cleymans[1], Helmut Oeschler[2] and Krzysztof Redlich[3,4]
[1]*Department of Physics, University of Cape Town, Rondebosch 7701, South Africa*
[2]*Institut für Kernphysik, Technische Universität Darmstadt, D-64289 Darmstadt, Germany*
[3]*Gesellschaft für Schwerionenforschung, D-64291 Darmstadt, Germany*
[4]*Institute for Theoretical Physics, University of Wrocław, PL-50204 Wrocław, Poland*
(February 9, 2008)

Attention is drawn to the role played by the size of the system in the thermodynamic analysis of particle yields in relativistic heavy ion collisions at SIS energies. This manifests itself in the non-linear dependence of K^+ and K^- yields in AA collisions at 1 – 2 A·GeV on the number of participants. It is shown that this dependence can be quantitatively well described in terms of a thermal model with a canonical strangeness conservation. The measured particle multiplicity ratios ($\pi^+/p, \pi^-/\pi^+, d/p, K^+/\pi^+$ and K^+/K^- but not η/π^0) in central Au-Au and Ni-Ni collisions at 0.8 – 2.0 A·GeV are also explained in the context of a thermal model with a common freeze-out temperature and chemical potential. Including the concept of collective flow a consistent picture of particle energy distributions is derived with the flow velocity being strongly impact-parameter dependent.

I. INTRODUCTION

It was pointed out by Hagedorn [1] some thirty years ago that thermal models overestimate the production of anti-He^3 in proton-proton collisions by seven orders of magnitude when the grand canonical ensemble is used in its standard form [2]. The reason for this is that when the number of particles as well as the interaction volume are small one has to take into account the fact that the production of anti-He^3 must be accompanied by the production of another three nucleons with energy E_N in order to conserve the baryon number. Thus, the abundance will not be proportional to the standard Boltzmann factor given by

$$n_{\overline{He^3}} \sim \exp\left(-\frac{m_{\overline{He^3}}}{T}\right) \tag{1.1}$$

but to

$$n_{\overline{He^3}} \sim \exp\left(-\frac{m_{\overline{He^3}}}{T}\right)\left[V\int\frac{d^3p}{(2\pi)^3}\exp\left(-\frac{E_N}{T}\right)\right]^3 \tag{1.2}$$

since three additional nucleons must be produced in order to conserve the baryon number. This suppresses the rate and introduces a cubic volume dependence. The original presentation of Hagedorn has been considerably developed and expanded in refs. [3–11].

Recently it has become clear that a similar treatment should be followed for strangeness production in the GSI/SIS energy range [12]. This is not only due to the fact that the size of the system is small but mainly because the temperature is very low and particle numbers are small. The abundance of K^+-mesons is then given by

$$n_{K^+} \sim \exp\left(-\frac{m_{K^+}}{T}\right)\left[g_{\overline{K}}V\int\frac{d^3p}{(2\pi)^3}\exp\left(-\frac{E_{\overline{K}}}{T}\right) + g_\Lambda V\int\frac{d^3p}{(2\pi)^3}\exp\left(-\frac{E_\Lambda}{T}\right)\right]. \tag{1.3}$$

since the strangeness must be balanced either by an anti-kaon or by a hyperon. g_i are the degeneracy factors and E_i the particle energies. This leads to a linear dependence of the K^+ density on the size of the system. Such a dependence has indeed been observed by the KaoS collaboration for K^+-mesons [13,14].

In this paper we would like to explore this idea in detail. This volume dependence can now be tested for the first time by considering the data on impact parameter dependence which are now becoming available.

In section II we review the thermal model with special emphasis on the canonical corrections due to the exact conservation of quantum numbers. In section III we present a comparison with the experimental data from SIS. One part is devoted to a systematic study of central collisions of various systems, another part to a detailed investigation of the impact-parameter dependence. The last section is devoted to a discussion of our results.

II. CONCEPTS AND PREDICTIONS

The exact treatment of quantum numbers in statistical mechanics has been well established for some time now [6]. It is in general obtained by projecting the partition function onto the desired values of the conserved charges by using the group theoretical methods (for a review see e.g. [7].) For our purpose we shall only consider the conservation laws related to the abelian U(1) symmetry group. In this case the formalism is particularly simple and leads to the following form of the canonical partition function for a fixed value of the conserved charge Q:

$$Z_Q = \frac{1}{2\pi}\int_0^{2\pi} d\phi e^{-iQ\phi}\tilde{Z}(T,V,\phi) \tag{2.1}$$

where $\tilde{Z}$ is obtained from the grand canonical (GC) partition function replacing the fugacity parameter λ_Q by the factor $e^{i\phi}$,

$$\tilde{Z}(T,V,\phi) \equiv Z^{GC}(T,V,\lambda_Q \to e^{i\phi}) \tag{2.2}$$

The particular form of the generating function $\tilde{Z}$ in the above equation is model dependent. Having in mind the applications of the statistical description to particle production in heavy ion collisions we calculate $\tilde{Z}$ in the ideal gas approximation, however, including all particles and resonances listed in [15]. This is not an essential restriction, because, describing the freeze-out conditions, we are dealing with a dilute system where the interactions should not influence particle production anymore. We neglect any medium effects on particle properties. In general, however, already in the low-density limit, the modifications of resonance width or particle dispersion relation, in this particular for Δ and π [16,17], cannot be excluded. For the sake of simplicity, we use classical statistics, i.e. we assume temperature and density regime so that all particles can be treated using Boltzmann statistics.

In nucleus-nucleus collisions the absolute values of baryon number, electric charge and strangeness are fixed by the initial conditions. Modeling particle production in statistical thermodynamics would, in general, require the canonical formulation of all these quantum numbers. ¿From the previous analysis [12], however, it is clear that only strangeness should be treated exactly, whereas the conservation of baryonic and electric charges can be described by the appropriate chemical potentials in the grand canonical ensemble.

Within the approximations described above and neglecting the contributions from multi-strange baryons, the generating function in equation (2.1) has the following form for a gas having zero total strangeness, $S = 0$:

$$Z_S(T,V,\mu_Q,\mu_B,\phi) = \exp(N_{s=0} + N_{s=1}e^{i\phi} + N_{s=-1}e^{-i\phi}) \tag{2.3}$$

where $N_{s=0,\pm1}$ is defined as the sum over all particles and resonances having strangeness $0, \pm1$,

$$N_{s=0,\pm1} = \sum_k Z_k^1 \tag{2.4}$$

and Z_k^1 is the one-particle partition function defined as

$$Z_k^1 \equiv \frac{Vg_k}{2\pi^2}\, m_k^2\, T\, K_2(m_k/T)\, \exp(b_k\mu_B + q_k\mu_Q) \tag{2.5}$$

with the mass m_k, spin-isospin degeneracy factor g_k, the particle baryon number b_k and electric charge q_k. The volume of the system is V and the chemical potentials related with the charge and the baryon number are determined by μ_Q and μ_B respectively.

With the particular form of the generating function equations (2.3,2.4,2.5) the ϕ-integration in equation (2.1) can be done analytically giving the canonical partition function for a gas with total strangeness S in the following compact form [10]:

$$Z_S(T,V,\mu_B,\mu_Q) = Z_0(T,V,\mu_B,\mu_Q) I_S(x) \tag{2.6}$$

where $Z_0 = \exp(N_{S=0})$ is the partition function of all particles having zero strangeness and the argument of the Bessel function

$$x \equiv 2\sqrt{S_1 S_{-1}}. \tag{2.7}$$

with $S_{\pm1} \equiv N_{s=\pm1}$.

The calculation of the particle density n_k in the canonical formulation is straightforward. It amounts to the replacement

$$Z_k^1 \mapsto \lambda_k \, Z_k^1 \tag{2.8}$$

of the corresponding one-particle partition function in equation (2.4) and taking the derivative of the canonical (C) partition function equation (2.1) with respect to the particle fugacity λ_k

$$n_k^C \equiv \lambda_k \, \frac{\partial}{\partial \lambda_k} \ln Z_Q(\lambda_k) \Big|_{\lambda_k = 1} \tag{2.9}$$

As an example, we quote the result for the density of thermal kaons in the canonical formulation assuming the total strangeness of the system $S = 0$,

$$n_K^C = \frac{Z_K^1}{V} \frac{S_1}{\sqrt{S_1 S_{-1}}} \frac{I_1(x)}{I_0(x)}. \tag{2.10}$$

Comparing the above formula with the result for thermal kaons density in the grand canonical ensemble, $n_K^{GC} = (Z_K^1/V) \exp(\mu_S/T)$, one can see that the canonical result can be obtained from the grand canonical one replacing the strangeness fugacity $\lambda_S \equiv \exp(\mu_S/T)$ in the following way:

$$n_K^C = n_K^{GC} \left(\lambda_S \mapsto \frac{S_1}{\sqrt{S_1 S_{-1}}} \frac{I_1(x)}{I_0(x)} \right). \tag{2.11}$$

In the thermodynamic limit both the canonical and the grand canonical formulation are equivalent. For a small system, however, the differences are large. This can be seen in the most transparent way when comparing two limiting situations: the large and small volume limit of equation (2.10) In the thermodynamic limit $V \to \infty$ the argument of the Bessel function $x \to \infty$, thus

$$\lim_{x \to \infty} \frac{I_1(x)}{I_0(x)} \to 1 \tag{2.12}$$

and the kaon density is independent of the volume of the system as expected in the grand canonical ensemble. On the other hand in the limit of a small volume we have

$$\lim_{x \to 0} \frac{I_1(x)}{I_0(x)} \to \frac{x}{2} \tag{2.13}$$

and the particle density is linearly dependent on the volume. It is thus clear that the major difference between the canonical and the grand canonical treatment of the conservation laws appears through different volume dependence of strange particle densities. The relevant parameter, F_S, which measures the deviations of particle multiplicities from their grand canonical result is determined by the ratio of the Bessel functions

$$F_S \equiv \frac{I_1(x)}{I_0(x)} \tag{2.14}$$

with the argument x defined in equation (2.7). In Fig. 1 we show the canonical suppression factor F_S as a function of the argument x. To relate the initial volume of the system to the number of participants we use the approximate relation $V \sim 1.9\pi A_{part}$. The corresponding values of x at SIS, AGS and SPS energies are calculated with the baryochemical potential and temperature extracted from the measured particle multiplicity ratios. The results in Fig. 1 show the importance of the canonical treatment of strangeness conservation at SIS energies. Here, the canonical suppression factor can be even larger than an order of magnitude. For central Au-Au collisions at AGS or SPS energies this suppression is not relevant any more and the (GC)-formalism is adequate. In general, one expects that the statistical interpretation of particle production in heavy ion collisions requires the canonical treatment of strangeness conservation if the CMS collation energy $\sqrt{s} < 2 - 3$ GeV. This is mainly because at these energies the freeze-out temperature is still too low to maintain large-argument expansion of the Bessel functions in equation (2.12).

At low temperatures one needs to take into account the width of resonances. This is because the number of pions coming from e.g. the decay of a Δ-resonance is increased by the width of the Δ. The approximation of the width by a delta function is therefore not justified since an appreciable number of particles come from the decay of resonances below the resonance mass. One therefore replaces the one-particle partition function in equations (2.4) and (2.5) by:

$$Z_R^1 = N\,\frac{V d_R}{2\pi^2}\,T\,\exp(b_k\mu_B + q_k\mu_Q)\int_{s_{min}}^{s_{max}} ds\,s\,K_2(\sqrt{s}/T)\,\frac{1}{\pi}\,\frac{m_R\Gamma_R}{(s-m_R^2)^2+m_R^2\Gamma_R^2} \tag{2.15}$$

where s_{min} is chosen to be the threshold value for resonance decay and $\sqrt{s_{max}} \sim m_R + \Gamma_R$. The normalization constant N is adjusted so that the integral over the Breit-Wigner factor gives one.

Within the above model, the particle densities depend on four parameters: the chemical potentials, μ_Q and μ_B, related with the (GC)-description of charge and baryon number conservation, the temperature T and the initial volume of the system appearing through the canonical treatment of strangeness conservation. Constraints on these variables arise from the isospin asymmetry measured by the baryon number divided by twice the charge, $B/2Q$. For an isospin symmetric system this ratio is simply 1, for Ni+Ni it is 1.04 while for Au+Au this ratio is 1.25.

We are thus left with three independent parameters. For simplicity, the volume V will be identified with the volume of the system created initially in AA collisions estimated from the atomic number of colliding nuclei and from the impact parameter by using geometric arguments. In particular we use the relation of the volume parameter and the number of participating nucleons as it was indicated in Fig. 1.

In the following section we will discuss to what extent the thermal model can be used to understand particle production in nucleus-nucleus collisions at SIS energies.

III. COMPARISON WITH EXPERIMENTAL RESULTS

This section is divided into three parts. In the first one we discuss the general trends found in thermal models. In particular we illustrate the sensitivity of particle ratios on the temperature, T, and on the baryon chemical potential, μ_B. In the second part we discuss particle ratios measured in central collisions and compare experimental results obtained at SIS with the expectations of the thermal model. This avoids the problem that different particle species might originate from different impact parameter regimes as it is the case with inclusive studies. The impact parameter dependence is studied in the third part of this section.

A. General Trends

¿From equations (2.10,2.12,2.13) one sees that at fixed temperature and chemical potentials the volume dependence of kaon multiplicity in the canonical and the grand canonical ensemble is as following:

$$\langle N_K\rangle \sim \begin{cases} V & : \quad V \mapsto \infty \quad \text{(GC)} \\ V^2 & : \quad V \mapsto 0 \quad\;\; \text{(C)}. \end{cases} \tag{3.1}$$

This effect is shown explicitly in Fig. 2 where the different particle ratios are calculated as a function of the radius of the system. In order to make the analysis more complete one needs, in addition, to take into account the contribution of resonance decays to particle production. We use all the known branching ratios as given in [15] to calculate the particle multiplicities shown in Fig. 2.

The ratio K^+/π^+ involves one strange particle, and according to equation (2.10) should show substantial dependents on volume. Indeed, it increases smoothly from zero up to the value given by the grand canonical ensemble. The increase is faster for higher temperature because the value of the argument x of the Bessel functions in equation (2.10) increases. In the K^+/K^- ratio two strange particles are involved and the volume effect cancels out exactly. However, for very small values of the volume, there are a few non-strange resonances that decay into kaon pairs or into a kaon and a hyperon, this leads to the sharp rise in the value of this ratio for increasing volumes before it flattens off and becomes volume independent. The ratio ϕ/π^+ involves only non-strange particles and therefore is independent of the size of the system. The same behavior is expected for η mesons which is treated as non-strange particle, too.

Figure 3 evidences the locations of the freeze-out temperature T_f and of the freeze-out μ_B^f yielding the various particle ratios. This figure shows also the sensitivity when varying their values within the limits occurring in the experimental results. Discussing these trends requires different treatment of strange and non-strange particles.

The interesting feature of the deuteron to proton ratio, d/p, and the pion to proton ratio, π^+/p, is that they allow a good determination of the range of the thermal parameters. The π^+/p curve in the $(T-\mu_B)$ plane shows a temperature saturation for large μ_B which establishes the upper limit of the freeze-out temperature T_f. On the other hand, the d/p ratio fixes the range of the freeze-out μ_B^f as it shows a steep dependence on the temperature. In addition, as seen in Fig. 3, the variations of 20-30% on the value of the d/p ratio give a very similar range in the $(T-\mu_B)$ plane, making this observable particularly useful for the extraction of the freeze-out parameters.

In the SIS-energy range one expects, in the thermal model, a different dependence of the strange and non-strange particle yields on the volume of the system. Consequently, the ratio of strange to non-strange particle leads to a strong variation of thermal parameters with the system size. In Fig. 4 we show the K^+/π^+ ratio for different volumes. As expected, changing the volume implies a substantial modification of the curve in the $(T - \mu_B)$ plane corresponding to a fixed value of the K^+/π^+ yields. Thus, calculating the strange to non-strange particle ratio requires additional care of the system size. In our approach, however, the volume is not treated as an additional parameter but is rather related with the number of participating nucleons in AA collisions. For a given system size the K^+/π^+ ratio clearly determines the lower limit of the freeze-out temperature. The curves in Fig. 3 are calculated for $R = 4$ fm. The K^+/K^- in Fig. 3 yield exhibits similar behavior as d/p, i.e. showing a very strong dependence on the temperature but a rather weak dependence on the baryon chemical potential, μ_B. This lines do not depend on the volume.

An analysis of particle production in heavy ion collisions within a thermal fireball model requires two experimentally measured ratios to fix the freeze-out parameters, T_f, μ_B^f, and knowledge of the number of participating nucleons, A_{part} to establish the size of the fireball. The knowledge of more particle ratios allows to test the concept of a unique freeze-out time. In the following section we compare the predictions of the thermal model with experimental results for central AA collisions at SIS energies.

B. Central collisions

In central collisions, the number of participating nucleons is maximal. However, experimental results for zero impact parameter, $b = 0$, are not directly measured. However, for many experiments good-quality impact-parameter results are available and an extrapolation to $b = 0$ can be performed. The results of this extrapolation are summarized in Table 1. We discuss below the different entries in this table.

The results in Table 1 for pions are obtained from [18–20]. For the ratio π^+/p we used results from inclusive measurements since it was established that the pion multiplicity divided by the number of participants, M_π/A_{part}, does not vary with A_{part} [18–21]. At Ni-Ni at 0.8 A·GeV π^- data are not available and $\pi^+ = \pi^-/1.2$ has been used to account for the isospin asymmetry. The K^+ results for Ni+Ni are from [14] which are in very good agreement with [22]. The K^+ yield rises strongly with centrality as shown in [14]. At 1.0 and 1.8 A·GeV the K^+/π^+ ratio was obtained by extrapolating to $b = 0$. At 0.8 A·GeV we scaled with the inclusive K^+/π^+ ratio between 1.0 and 0.8 A·GeV. The impact-parameter dependence for K^- and K^+ is nearly identical [14] and we used therefore the K^+/K^- ratio of the inclusive measurements. The multiplicity of K^+ divided by the number of participants, M_{K^+}/A_{part}, in Au+Au increases strongly with impact-parameter as shown in [13,23]. The π^-/π^+ ratios show – if at all – only a very slight increase with centrality [20,24] and Table 1 summarizes the results for inclusive studies. These values in [20,24] agree very well with the isobar model. The ratios of d/p obtained in Ni+Ni are from [25] and those for Au+Au have been taken from [26]. The ratios η/π^0 for Ni+Ni are from [27,28]. At 1 A·GeV Ni+Ni has not been measured, yet Ar+Ca and Kr+Zr yield the equal ratios taking then also for Ni+Ni, at 0.8 A·GeV only Ar+Ca has been studied and this value is given in Table 1. The value at 1.8 A·GeV has been obtained by interpolation between 1.0 and 1.93 A·GeV. For Au+Au the results from [27] have been corrected for the increase with centrality according to [29].

Figure 5 shows the lines in the $(T - \mu_B)$ plane corresponding to the measured particle ratios in Au-Au collisions at 1 A·GeV. The experimental errors are for simplicity not shown in the figure. All lines, except the one for η/π^0, have a common crossing point around $T \sim 50$ and $\mu_B \sim 822$ MeV. A value of $R \sim 6.2$ fm is needed to describe the measured K^+/π^+ ratio with the freeze-out parameters extracted for π^+/p, π^+/π^- and d/p. This radius corresponds to $A_{part} \sim 330$ participating nucleons and is compatible with the one expected for central Au-Au collision.

The strangeness suppression due to the canonical treatment of the conservation laws is very clear in the comparison of the thermal model with the Au-Au 1 A·GeV data. Using the *grand canonical* formulation of the strangeness conservation one would get the value $K^+/\pi^+ \sim 0.04$ which overestimates the data by more than an order of magnitude. This shows that the conditions for thermal particle phase space at SIS energies are far from the grand canonical limit.

In Fig. 6 we show the corresponding results in the $(T - \mu_B)$ plane for Ni-Ni collisions at three different incident energies: 1.8, 1.0 and 0.8 A·GeV. As for the Au-Au data we see in Fig. 5 that all particle ratios, besides η/π^0 can be described by the same values of the freeze-out parameters. We notice the smaller radius of ~ 4 fm which is compatible with the smaller size of Ni. The measured K^+/K^- ratio leads to a band in the $(T - \mu_B)$ plane which barely misses the common crossing point for the mean values of π^+/p, d/p and K^+/π^+. However, taking into account the experimental errors on the above particle ratios leads to a common, narrow $(T - \mu_B)$-band which contains also the line corresponding to the upper experimental limit for $K^+/K^- \sim 30$. Allowing for a drop in the K^- mass as proposed in model calculations [30–32] leads to a shift of the K^+/K^- band towards the left in Fig. 6, thus leading to a better agreement with the other data. New experimental results on the K^+/K^- ratio also for other collision systems are needed to clarify this open question.

The values for the of d/p ratio shown in Fig. 6 for Ni-Ni collisions at 0.8 A·GeV were obtained by extrapolating the experimental measurements at E/A=1.06, 1.45, 1.93 summarized in Table 1 using a linear and a polynomial fit giving the value $d/p = 0.4, 0.43$. As one can see the 10% deviation on d/p ratio does not modify substantially the freeze-out line in the $(T - \mu_B)$ plane.

The results of Figs. 5, 6 show that for central Au-Au and Ni-Ni collisions the particle ratios, π^+/p, K^+/π^+, π^+/π^-, K^+/K^- and d/p, lead to a common crossing point in the $(T - \mu_B)$ plane. The appearance of the common freeze-out for all these particles is strong support for chemical equilibrium of these particles in the thermal model.

In Fig. 7 we show the results for the freeze-out temperature and chemical potential corresponding to different incident energies. It can be seen that the freeze-out temperature T_f increases with E/A whereas μ_B^f shows the opposite trend. In the energy range considered this dependence can be approximated by a straight line. The freeze-out parameters are also seen in Fig. 7 to be different in Ni-Ni and Au-Au collisions even for the same incident energy. It is interesting to remark that at a given incident energy the extracted values of T_f are smaller for central Au-Au collisions than for central Ni-Ni ones.

Using the freeze-out parameters relevant for SIS energies we can compare the results with the previous findings for AGS [33,34] and SPS [35–38] energies. The chemical freeze-out points in the $(T - \mu_B)$ plane for relativistic heavy ion collisions are shown in Fig. 8 together with the predictions for e^+e^- and p-p collisions [39]. Connecting these points leads to a unique freeze-out curve in the $(T - \mu_B)$ plane [40,41]. It has been shown [42] that the energy per hadron along the freeze-out curve (before the final decay of the hadron) is approximately 1 GeV.

It is a common feature of Figs. 5 and 6 that the freeze-out line for η production does not cross the common chemical freeze out extracted for all the other particle species. This deviation does not arise from the selection of central collisions. Only for Au-Au collisions we have chosen the η/π^0 ratio of central collisions. In the Ni-Ni system – due to the lack of experimental results – inclusive values are given. For central Ni-Ni collisions the discrepancy would therefore increase. The results in [29] show that the η yield rises more than linearly with A_{part}. This disagrees also with the expectations from the thermal concept discussed along with Fig. 2.

The problem of η abundance in the thermal model could have several origins. One possibility would be due to the sequential freeze-out for different particle species. Here, η could be produced earlier with higher temperature, roughly corresponding to the value obtained from the transverse momentum slope parameter of 80 MeV. In this case, as seen in Fig. 6, the large value of the η/π^0 ratio can be understood. In recent works [24,43,44] experimental evidence is given that high-energy pions are emitted earlier than those with lower energies. This points towards a span in freeze-out times but does not affect the particle ratios which are dominated by low-energy pions. The concept of sequential freeze-out, however, might lead to a problem with the interpretation of all other particle ratios which are otherwise well described by the model. We stress that the same thermal model when applied to AGS and SPS energies explains particle productions there with a single set of freeze-out parameters for all particles including η at SPS energies. It seems rather difficult to argue the appearance of a sequential freeze-out at SIS and its absence at AGS and SPS energies.

The discrepancy of the thermal model on the level of η production could possibly be related to the hidden strangeness content of the η meson. The crucial difference in the thermal model interpretation of particle production at SPS, AGS and SIS energies is due to the canonical strangeness suppression. In our formalism the η is considered as a non-strange particle. It is conceivable that due to hidden strangeness there should be corrections to the η yield from the canonical strangeness conservation. We do not know, yet, however, how these corrections could be included in a consistent way. The same arguments would apply also for the production of ϕ. Yet, ϕ/K^- (inclusive) seems to fit into the common crossing shown for Ni-Ni at 1.8 A·GeV. The large η yield could well be of dynamical origin which apriori cannot be explained by the thermal freeze-out model applied in this work. Thus, we leave the discrepancy of η production as an unsolved puzzle in the thermal model.

Concluding this part, we find that the thermal model gives a consistent description of both strange and non-strange particle production in central nucleus - nucleus collisions at SIS energies with the exception of the η/π^0 ratio. There is a serious problem with the understanding of this ratio in terms of the thermal model. Theory and experiment deviate by a factor of 2 to 8, depending on the incident energy. The same problem has been indicated recently in the context of dynamical model for pion and η production [16]. We would like to point out that recent transport-model calculations reproduce the measured η and π^0 spectra [45]. We would also like to draw attention to the systematics introduced by V. Metag in which pions and η's exhibit a common trend while K^+, K^- and ϕ show lower yields [46].

To check further the consistency of the model with the experimental data the impact parameter dependence of particle production and particle spectra are discussed in the next section.

C. Impact Parameter Dependence

As already mentioned, the multiplicity of K^+ divided by the number of participants, K^+/A_{part}, increases strongly with the centrality while the corresponding ratio for pions, K^+/A_{part}, is constant [14]. Consequently, the pion yield is proportional to the number of nucleons in the initially created fireball while the multiplicity of K^+ scale with A_{part} like $K^+ \sim A_{part}^{\alpha}$ with $\alpha > 1$. The experimental results on K^+/π^+ and K^+/A_{part} ratios in Au-Au collisions from Ref. [23] are shown in Fig. 9. The canonical treatment of strangeness conservation predicts the yield of strange particles to increase quadratically with the number of participants (see eq. (2.14)). An additional complication is due to the possible variation of the freeze-out parameters with centrality.

In Fig. 9 the dashed-line describes the results of the thermal model under the assumption that both T_f and μ_B^f are A_{part} independent. One sees that already under this simple approximation the agreement of the model and the experimental data is very satisfactory. The small deviations between the model and the data can be accounted for by the variation of the freeze-out parameters with A_{part}.

We have calculated the possible change of T_f and μ_B^f with A_{part} from the experimental data on K^+/π^+ and d/p ratios measured for two different values of A_{part} (see Fig. 10). The resulting freeze-out parameters are shown in Fig. 11. One can see that the variation of T_f and μ_B^f with A_{part} are small. It is interesting to note that peripheral collisions yield higher temperatures than central collisions. The results from central $Ni-Ni$ collisions fit perfectly into the trend with A_{part}.

In Fig. 9 the dashed-dotted lines were obtained parameterizing the T_f and μ_B^f dependence on A_{part} using the small variation in freeze-out parameters obtained from Fig. 11. The shape of the experimental data is now well reproduced.

The rather small variation of the freeze-out temperature with impact parameter shown in Fig. 11 comes as a surprise since the experimental results on the apparent inverse slope parameter T_{app} of particle yields shows a strong dependence on A_{part}. The freeze-out temperature of ~ 50 MeV derived from our analysis is also substantially lower than the value previously obtained from the particle spectra [18–20,25,44,47,48].

We now turn our attention to the differential cross sections for particle production. In Fig. 12 we show the variation of the inverse slope parameters observed for various particle species [18,25]. Yet, adopting our result, that there exists a common, impact-parameter independent, freeze-out temperature for all particles one needs to show that the variation in slope results from radial flow varying with impact parameter. We extract the values of the corresponding flow parameters β using the Siemens-Rasmussen formula [49]. The resulting values for the flow velocity, β, are summarized in Fig. 12. With the freeze-out temperature $T_f \sim 50$ MeV the spectra of p, K^+ and π^+ are, within the experimental uncertainty, well explained with the same β as shown in Fig. 12. The variation of β with impact parameter turns out to be very large.

The A_{part} dependence of various particle yields ($Y \sim A_{part}^{\alpha}$) has been discussed in [18] and the exponent α has been suggested to be related with the difference in total energy needed for the production of the studied particle and the one available in NN collisions. In the presented concept the exponent α is only due to volume-dependent strangeness suppression. In this picture the exponent for K^+ and for K^- production is predicted to be equal while in the frame of the energy argument [18] α should be higher for K^- than for K^+ due to different production thresholds (neglecting in-medium mass modifications). It is clear that any non-isotropic emission pattern is beyond the scope of this model. However, – as naively expected – the slopes of K^+ and of K^- do not have to be equal as different resonance decays contribute.

The results of this section show that the thermal model gives a consistent picture for particle production in AA collisions at SIS energies. In addition to the correct predictions for particle yields the model can also explain the A_{part} dependence of K^+ cross section. Assuming radial flow as an origin of the shape of particle spectra one can understand quantitatively the inverse slopes with a common temperature and radial flow velocity for all particles. The chemical and thermal freeze-out seem to be very close at SIS energies. This is because the particle multiplicities and momentum spectra can be explained with the same temperature.

IV. SUMMARY

In summary, the thermal model provides a remarkably consistent description of the experimental data in the GSI/SIS energy range. The abundances of particles, K^+, K^-, p, d, π^+ and π^- (with the notable exception of η's) seem to come from a common hot source with a surprisingly well defined temperature, $T \approx 50, 54, 70$ MeV, and baryon chemical potential $\mu_B \approx 825, 805, 750$ MeV for central Ni-Ni at 0.8, 1.0, 1.8 A·GeV and correspondingly $T \approx 52$ MeV and $\mu_B \approx 822$ MeV for central Au-Au collisions at 1.0 A·GeV, as can be seen clearly from Figs. 5,7 and 8. These temperatures are lower than the ones observed in the particle spectra but here again a common explanation is possible in terms of hydrodynamic flow. Flow differentiates between heavy and light particles since they acquire

the same boost in velocity but of course very different kicks in momenta. This is clearly seen in the GSI/SIS data shown in Fig. 12 which also summarize the transverse flow velocity for pions, kaons and protons.

The common crossing points exhibited in Figs. 5, 6 are a very strong argument for chemical equilibrium. The deviations found for the production of η mesons clearly ask for an explanation.

V. ACKNOWLEDGMENTS

We acknowledge stimulating discussions with R. Averbeck, P. Braun-Munzinger, B. Friman, V. Metag, W. Nörenberg and W. Weinhold.

---

[1] R. Hagedorn, CERN yellow report 71-12 (1971).
[2] For a recent review of $\overline{He^3}$ production see P. Sonderegger, R.Shahoian, S. Albergo in "*Critical Phenomena and Collective Observables*", Proc. of CRIS'96, 1st Catania Relativistic Ion Studies, Acicastello, May 27-31, 1996, World Sci., p. 225.
[3] R. Hagedorn and K. Redlich, *Z. Phys.* A **27**, 541 (1985).
[4] K. Zalewski, Acta Phys. Pol. 28, (1965) 933; E. M. Ilgenfritz, and J. Kripfganz, *Nucl. Phys.* B **62**, 141 (1973).
[5] J. Rafelski and M. Danos, *Phys. Lett.* B **97**, 279 (1980).
[6] K. Redlich and L. Turko, *Z. Phys.* C **5**, 201 (1980); L. Turko, *Phys. Lett.* B **104**, 361 (1981).
[7] B. Müller, " *The Physics of the Quark-Gluon Plasma*", pp. 91-104, Lecture Notes in Physics 225, Springer-Verlag (1985).
[8] C. Derreth, W. Greiner, H.-Th. Elze and J. Rafelski, *Phys. Rev.* C **31**, 360 (1985).
[9] M. Gorenstein, V.K. Petrov and G.M. Zinovjev, *Phys. Lett.* B **106**, 327 (1981).
[10] J. Cleymans, K. Redlich and E. Suhonen, *Z. Phys.* C **51**, 137 (1991).
[11] J. Cleymans, E. Suhonen, G.M. Weber, *Z. Phys.* C **53**, 485 (1991).
[12] J. Cleymans, D. Elliott, A. Keränen and E. Suhonen, *Phys. Rev.* C **57**, 3319 (1998)
[13] D. Miśkowiec et al., *Phys. Rev. Lett* **72**, 3650 (1994).
[14] R. Barth et al., (KaoS collaboration), *Phys. Rev. Lett* **78**, 4007 (1997).
[15] C. Caso et al. (Particle Data Group), *Eur. Phys. Jour.* C3,1 (1998).
[16] W. Weinhold, B. Friman, W. Nörenberg, *Phys. Lett.* B **433**, 236 (1998).
[17] E.E. Kolomeitsev, D.N. Voskresensky, B. Kämpfer, *Int. J. of Mod. Phys. E* Vol. 5, 313 (1996).
[18] C. Müntz et al., (KaoS collaboration), *Z. Phys.* A **357**, 399 (1997).
[19] D. Pelte et al., (FOPI collaboration), *Z. Phys.* A **357**, 215 (1997).
[20] D. Pelte et al., (FOPI collaboration), *Z. Phys.* A **359**, 55 (1997).
[21] J.W. Harris et al., *Phys. Rev. Lett* **58**, 463 (1987).
[22] D. Best et al., (FOPI collaboration), *Nucl. Phys.* A **625**, 307 (1997).
[23] M. Mang, (KaoS collaboration), PhD Thesis (1997), University of Frankfurt , Germany.
[24] A. Wagner et al., (KaoS collaboration), *Phys. Lett.* B **420**, 20 (1998).
[25] B. Hong et al., (FOPI collaboration), *Phys. Rev.* C **57**, 244 (1998).
[26] H. Pöppl, (KaoS collaboration), PhD Thesis (1993), University of Marburg, Germany.
[27] R. Averbeck et al., (TAPS collaboration) TAPS workshop, St. Odile, Sept. 1997 nucl-ex/9803001.
[28] A. Marín et al., (TAPS collaboration), *Z. Phys.* A **341**, 123 (1997).
[29] A.R. Wolf et al., (TAPS collaboration), *Phys. Rev. Lett* **80**, 5281 (1998)
[30] J. Schaffner, J. Bondorf and I. Mishustin, *Nucl. Phys.* A **625**, 325 (1997).
[31] Q.G. Li, C.H. Lee and G.E. Brown, *Nucl. Phys.* A **625**, 372 (1997).
[32] T. Waas, N. Kaiser, W. Weise, *Phys. Lett.* B **379**, 34 (1996); T. Waas, M. Rho and W. Weise, *Nucl. Phys.* A **617**, 44 (1997).
[33] P. Braun-Munzinger, J. Stachel, J.P. Wessels and N. Xu, *Phys. Lett.* B **344**, 43 (1995).
[34] J. Cleymans, D. Elliott, R. L. Thews, and H. Satz, *Z. Phys.* C **74**, 319 (1997).
[35] J. Sollfrank, J. of Physics G23, (1997) 1903.
[36] R. Stock, *Nucl. Phys.* A **630**, in print (1998).
[37] J. Cleymans, 3rd International Conference on "Physics and Astrophysics of Quark-Gluon Plasma", Jaipur, India, March 17 - 21, 1977 to be published, nucl-th/9704046.
[38] F. Becattini, M. Gaździcki, and J. Sollfrank, *Eur. Phys. Jour.* C5, 143 (1998).
[39] F. Becattini, *Z. Phys.* C **69**, 485 (1996); F. Becattini, and U. Heinz, *Z. Phys.* C **76**, 269 (1997).
[40] R. Hagedorn and J. Rafelski, *Phys. Lett.* B **97**, 136 (1980).

[41] P. Braun-Munzinger, J. Stachel, J.P. Wessels and N. Xu, *Phys. Lett.* B **365**, 1 (1996); P. Braun-Munzinger, and J. Stachel, Nucl. Phys. A606, (1996) 320; nucl-ex/9803015, Nucl. Phys. A (1998) *in print.*
[42] J. Cleymans and K. Redlich, GSI-preprint No. 98-43, /nucl-th9808030 (1998).
[43] A. Wagner, (KaoS collaboration), PhD Thesis (1996), Technical University Darmstadt, and to be published.
[44] H. Oeschler, (KaoS collaboration), presented at the 11th Chris Engelbrecht Summer School in Theoretical Physics, "Hadrosynthesis and Hadrons in Dense Matter", Cape Town 4-13 February 1998, (to be published in "Lecture Notes in Physiscs", Springer Verlag).
[45] E.L. Bratkovskaya et al., *Nucl. Phys.* A **634**, 168 (1998).
[46] V. Metag, *Prog. Part. Nucl. Phys.* 30, 75 (1993); V. Metag, GSI-Preprint 97-43.
[47] N. Herrmann, (FOPI collaboration), *Nucl. Phys.* A **610**, 49c (1996).
[48] M. Appenheimer et al., (TAPS collaboration), GSI 97-1, page 58; R. Averbeck, "Hadronische Materie bei SIS-Energien - Eine Thermodynamische Analyse." (unpublished), presented at the DPG Frühjahrstagung, Göttingen, February 1997.
[49] P. J. Siemens and J. O. Rasmussen, *Phys. Rev. Lett* **42**, 880 (1989).

Reaction	E A·GeV	π^+/p	K^+/π^+	π^-/π^+	d/p	K^+/K^{-a}	η/π^0
Ni+Ni	0.8	0.05	0.0003				*0.004*
Ni+Ni	1.0	0.08	0.001	*1.2*	0.37		*0.013*
Ni+Ni	1.8	0.17	0.0084	*1.05*	0.28	21±9	*0.03*
Au+Au	1.0	0.052	0.003	2.05*(1.94)*			0.03/*0.014*

TABLE I. *Experimental results for different particle ratios in central AA collisions. Values in italics are for inclusive measurements. The errors are estimated to 20 – 30 %.*

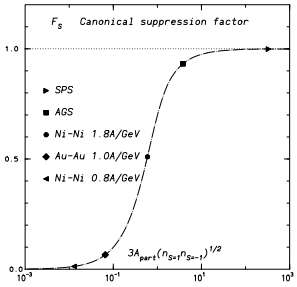
F_S Canonical suppression factor
1.0
0.5
0.0
10^{-3}
10^{-1}
10^{1}
10^{3}
SPS
AGS
Ni-Ni 1.8A/GeV
Au-Au 1.0A/GeV
Ni-Ni 0.8A/GeV
$3A_{part}(n_{S=1}n_{S=-1})^{1/2}$

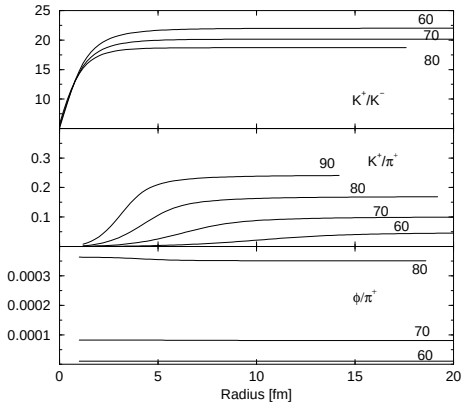
25
20
15
10
60
70
80
K+/K−
0.3
0.2
0.1
90
K+/π+
80
70
60
0.0003
0.0002
0.0001
80
φ/π+
70
60
0
5
10
15
20
Radius [fm]

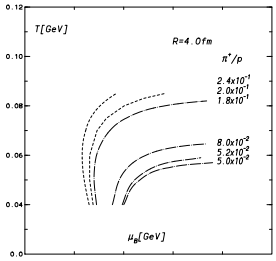
T[GeV]
R=4.0fm
π⁺/p
2.4x10⁻¹
2.0x10⁻¹
1.8x10⁻¹
8.0x10⁻²
5.2x10⁻²
5.0x10⁻²
μB[GeV]

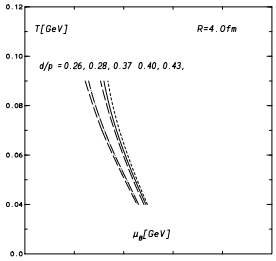
T[GeV]
R=4.0fm
d/p =0.26, 0.28, 0.37 0.40, 0.43,
μB[GeV]

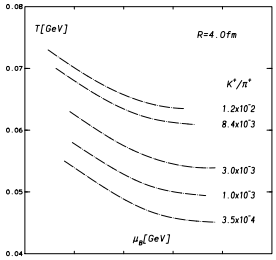
T[GeV]
R=4.0fm
K⁺/π⁺
1.2x10⁻2
8.4x10⁻3
3.0x10⁻3
1.0x10⁻3
3.5x10⁻4
μB[GeV]

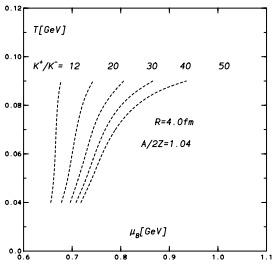
T[GeV]
K+/K- = 12
20
30
40
50
R=4.0fm
A/2Z=1.04
μB[GeV]
0.12
0.10
0.08
0.06
0.04
0.0
0.6
0.7
0.8
0.9
1.0
1.1

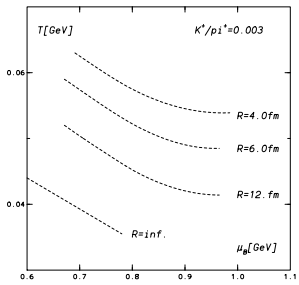
T[GeV]
K+/pi+=0.003
0.06
0.04
R=4.0fm
R=6.0fm
R=12.fm
R=inf.
μB[GeV]
0.6
0.7
0.8
0.9
1.0
1.1

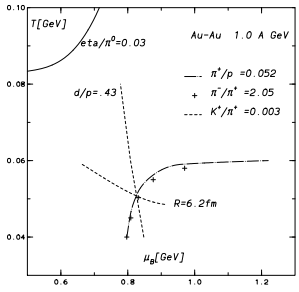
T[GeV]
eta/π⁰=0.03
d/p=.43
Au-Au 1.0 A GeV
π⁺/p =0.052
π⁻/π⁺ =2.05
K⁺/π⁺ =0.003
R=6.2fm
μB[GeV]
0.10
0.08
0.06
0.04
0.6
0.8
1.0
1.2

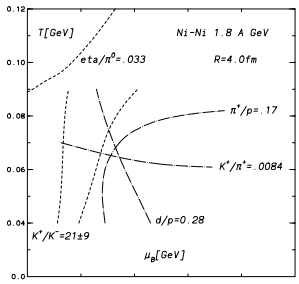
T[GeV]
Ni-Ni 1.8 A GeV
eta/π⁰=.033
R=4.0fm
π⁺/p=.17
K⁺/π⁺=.0084
d/p=0.28
K⁺/K⁻=21±9
μB[GeV]
0.12
0.10
0.08
0.06
0.04
0.0

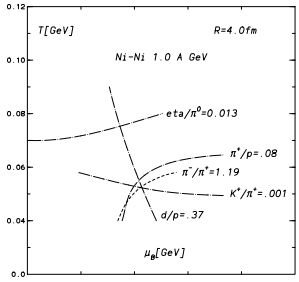
T[GeV]
R=4.0fm
Ni-Ni 1.0 A GeV
eta/π⁰=0.013
π⁺/p=.08
π⁻/π⁺=1.19
K⁺/π⁺=.001
d/p=.37
μB[GeV]
0.12
0.10
0.08
0.06
0.04
0.0

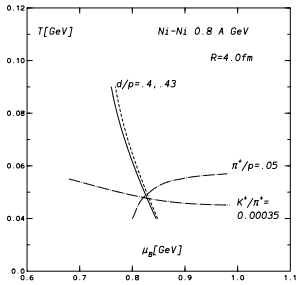
T[GeV]
Ni-Ni 0.8 A GeV
R=4.0fm
d/p=.4,.43
π+/p=.05
K+/π+=
0.00035
μB[GeV]
0.12
0.10
0.08
0.06
0.04
0.0
0.6
0.7
0.8
0.9
1.0
1.1

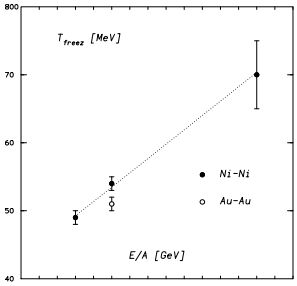
800
70
60
50
40
T_{freez} [MeV]
Ni-Ni
Au-Au
E/A [GeV]

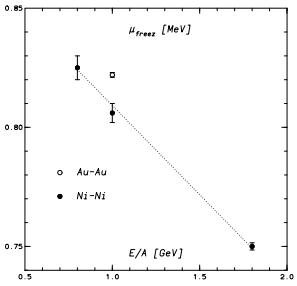
0.85
0.80
0.75
0.5
1.0
1.5
2.0
μ_{freez} [MeV]
Au-Au
Ni-Ni
E/A [GeV]

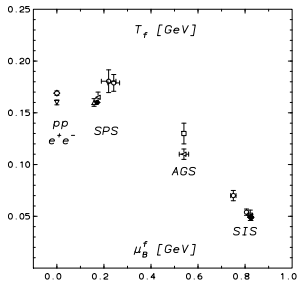
T_f [GeV]
pp
e^+e^-
SPS
AGS
SIS
μ_B^f [GeV]
0.25
0.20
0.15
0.10
0.05
0.0
0.2
0.4
0.6
0.8
1.0

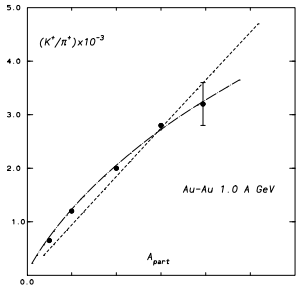
$(K^+/\pi^+)x10^{-3}$
Au-Au 1.0 A GeV
A_{part}

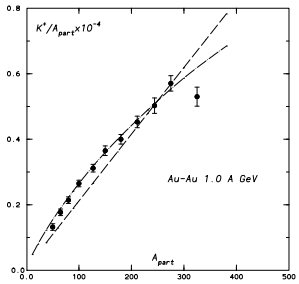
$K^+/A_{part}x10^{-4}$
Au-Au 1.0 A GeV
A_{part}

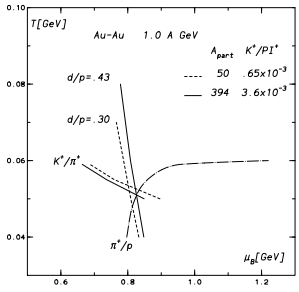
T[GeV]
Au-Au 1.0 A GeV
A_part K+/Pi+
---- 50 .65x10^-3
—— 394 3.6x10^-3
d/p=.43
d/p=.30
K+/π+
π+/p
μB[GeV]
0.10
0.08
0.06
0.04
0.6
0.8
1.0
1.2

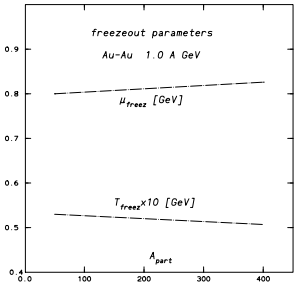
freezeout parameters
Au-Au 1.0 A GeV
μ_{freez} [GeV]
T_{freez}x10 [GeV]
A_{part}
0.9
0.8
0.7
0.6
0.5
0.4
0.0
100
200
300
400

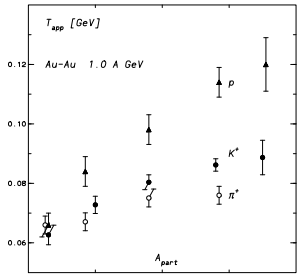

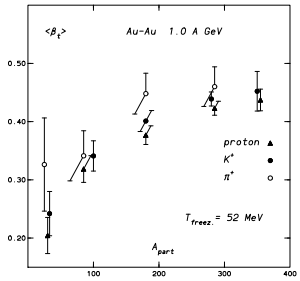

VI. FIGURE CAPTION

Fig.1 *Canonical strangeness suppression factor (see text).*

Fig.2. *Dependence of various particle ratios on the radius parameter R.*

Fig.3 *General trends for* π^+/p, d/p, K^+/π^+ *and* K^+/K^- *freeze-out curve calculated with* $R = 4.0$ *fm and isospin asymmetry corresponding to* $A/2Z = 1.04$.

Fig.4 *Dependence of* K^+/π^+ *freeze-out line with the radius R ..*

Fig.5 *Freeze-out lines corresponding to different particle ratios measured in Au+Au collisions at 1 A·GeV.*

Fig. 6 *T versus μ_B for central Ni+Ni collisions from 0.8 to 1.8 A·GeV.*

Fig.7 *Freeze-out T_f and μ_B^f as a function of incident energy as extracted from the common crossing in Figs. 5, 6 – neglecting the results from η/π^0.*

Fig.8 *Freeze-out parameters T_f and μ_B^f for SPS, AGS and SIS energies.*

Fig.9 *Measured K^+/π^+ and K^+ multiplicity per A_{part} as a function of A_{part} for Au+Au at 1 A·GeV together with two calculations (see text).*

Fig.10 *Freeze-out parameters T and μ_B for different A_{part}.*

Fig.11 *Variation of freeze-out parameters T and μ_B as a function of A_{part}.*

Fig.12 *Apparent temperatures for p, π^+, K^+ (data from [23]) and calculated flow velocities as a function of A_{part} for Au+Au at 1 A·GeV.*